

Electron free energy levels in oxidic solutions: relating oxidation potentials in aqueous and non-aqueous systems

C. A. Angell

Received: 4 September 2008 / Revised: 16 December 2008 / Accepted: 17 December 2008
© Springer-Verlag 2009

Abstract We provide background to the problem of describing the state of redox couples in different types of solvent media ranging from acidic aqueous solutions to high temperature molten silicates, pointing out the essential similarity between these solvent media in Lewis acid–base terms. We review the adaptation of the Gurney proton energy level diagram approach to the case of electron transfer processes. Using data from various spectroscopic and analytical chemistry sources, we review the construction of electron free energy level diagrams for redox couples in aqueous and non-aqueous systems using, as a common reference, the potential of the oxygen gas (1 atm)/oxide ion couple in the solution of interest. We emphasize the anomalous effect of “oxide ion activity” (mean ionic activity of alkali oxide) on the state of equilibrium and interpret this in terms of oxide ion transfers that accompany electron transfers. After showing the essential agreement between recent direct electrochemical assessments of the energy levels and those deduced in our original analysis of oxidic melts of different glass formers, we provide an interpretation of the apparent “oxide ion transfer” in terms of the differential medium polarization by the two redox species involved in the equilibrium. We anticipate the extension of these ideas to redox chemistry in the currently burgeoning field of “ionic liquids” in its recent *ambient temperature liquid* incarnation.

Introduction

John Bockris pioneered the application of modern ideas about ionic substances to the case of silicate liquids and was the first to use the term “ionic liquids” for their description. His papers with Lowe [1], McKenzie [2], Kitchener [2, 3], and Tomlinson [3, 4] on this subject are now classics. In rather separate studies, he made great contributions to the electrochemical sciences, pioneering with Parsons and Conway [5] the strategies for electrochemical purifications, among a great many other developments. These latter works were focused on applications involving aqueous solutions, though they relate equally to purification of molten salts, polymer electrolytes, and liquid silicates. The electrochemistry of molten salts, if not liquid silicates, is a subject of great current importance in relation to the technology of nuclear fuel reprocessing [6].

In liquid silicates, redox chemistry has always been of great importance in the winning of metals from ores, but the electrochemical conditions of importance have been determined more by oxygen pressure variations controlled by carbon chemistry than by direct electrochemical interrogation. Electrochemical studies of redox potentials have been more recent. Most of the redox potentials in non-aqueous solutions discussed by us long ago [7] and now reproduced in this paper were gleaned from chemical equilibrium studies (at fixed oxygen pressure established by bubbling gases), e.g., [9–12], rather than the inverse process where the chemical concentrations are fixed by the experimentalist and the potentials then directly measured [13, 14]. The latter approach is best illustrated by the recent work of Rüssel and co-workers using square wave voltammetry [15–18], to be discussed further below.

We became interested in the redox chemistry of species in silicate, borate, and phosphate liquids through the

Dedicated to the 85th birthday of John O’M. Bockris.

C. A. Angell (✉)
Department of Chemistry and Biochemistry,
Arizona State University,
Tempe, AZ 8528, USA
e-mail: austenangell@gmail.com

absorption spectra of transition metal ions that may be dissolved in them [19, 20], some of which (Ni^{2+} and Co^{2+}) provided useful probes for the likely local structures around important liquid silicate cations like Mg^{2+} and Zn^{2+} . The attractive feature of transition metal ion spectroscopy lies in the precision of the structural information that the spectra convey [21] and the richness of structural variation that can then be deduced from the changes in electronic absorption lines that accompany changes in silicate melt structure. These changes can themselves be controlled by chemical composition, specifically by the oxide oxygen-to-Si ratio, which in turn determines the activity of oxide ions (more precisely, the mean ionic activity of the basic oxide, such as Na_2O , that is being used to donate oxide ions to the disruption of the initially polymeric silica network).

As our work in this area proceeded, particularly the aspect driven by the need to produce a coherent body of work under the title *Glass: structure by spectroscopy* [7] (the book co-authored with friend and colleague Joe Wong), we became impressed by the essential similarity of redox equilibria witnessed in high temperature liquid silicates via absorption spectroscopy and those seen by electrochemical measurements in aqueous solutions. This similarity [7] has been given little attention in the literature since that time but has recently been noticed also by Duffy and Ingram [22]. However, the relevance of the Pourbaix type diagram for redox equilibria, developed in such detail for aqueous solutions and adopted by us for the case of silicate melts, seems to have been completely neglected in subsequent work. Given the current success of direct electrochemical measurements on oxide melts [15, 18], the failure to utilize such a useful and economic graphical summary of the redox equilibria characteristic of a given solvent as the Pourbaix diagram leaves a serious gap in the field, as we will review.

A key insight from our earlier study of this problem concerned the reasons *why* highly basic environments in melts tend to favor the higher oxidation states in any given system. This was given particular emphasis in [23], which, isolated in an obscure symposium volume, has received little attention. While the more recent literature contains abundant confirmation of this trend [18, 24], there has been little concomitant development beyond, or even commentary on, our essentially simple interpretation of this trend. Since this insight seems to be missing from other publications in the solutions area, we give it some emphasis in this paper, reproducing much directly from [23]. The present paper then represents a revisiting of this phenomenology with a commentary on the progress that has been made during the 40 years of research since the publication of *Glass: structure by spectroscopy*.

We begin with some observations intended to make molten silicate and aqueous solutions seem less different than they might appear at first sight.

The familiar “basic” solution of aqueous solution chemistry is produced by reacting the strong Lewis base, Na_2O , with the weak Lewis acid, H_2O , initially to produce, by proton transfer, the “neutral” compound NaOH . To this product is then added a large excess of the acid component (55.5:1 molar ratio for a one molar solution). In an exactly analogous fashion, an ordinary sodium silicate glass is produced by reacting the same Lewis base Na_2O with the Lewis acid SiO_2 , initially to form the neutral compound, Na_4SiO_6 , to which is then added a large excess of the acid component. It is not surprising then that the chemistry of the two types of acid–base systems should have common features¹: Both are characterized by very low values of the mean oxide activity $a_{\pm}^{\text{Na}_2\text{O}}$. At ambient temperatures, of course, one of the systems is a solid glass, hence out of equilibrium, while the other is mobile equilibrated solution (see footnote 1). However, the equilibria in the silicate systems were established at high temperatures in equilibrium with an air atmosphere, at $p\text{O}_2 = 0.2$ atm (which requires a gas bubbler, to be reliable), and when the liquid is quenched, the redox equilibria are trapped in for subsequent ambient temperature study [the slowness of equilibration with stagnant atmospheres has not always been recognized, and where discrepancies between direct electrochemical and spectrophotometric (or chemical analysis-based results occur), this is a likely cause].

We note that, while fundamental silicate solution studies have mostly been carried out with sodium silicate solutions, practical glasses, e.g., “window” glass, require a certain amount of the weaker base CaO to be included for the very practical reason that the pure sodium silicate solution is rather soluble in water. Because it is not a common consideration in aqueous chemistry, it is useful to point out in this study that the oxide activity sensed by the redox species in oxidic solutions is very much dependent on the nature of the cations that accompany the basic oxide that reacts with the Lewis acid to generate the solution. In the field of geochemistry and also in the science of zero expansivity materials, the aluminum cation is important.

A number of recent studies permit us to view the effect of these cations on the “oxide activity” of melts through their effect on the potentials of various redox couples [18]. These are generally consistent with the conclusions to be drawn from the well-known work of Duffy and Ingram [25–29] in which a spectroscopic method of assessing the activity of the oxide ion in melts and glasses is used. Duffy and Ingram used the ultraviolet spectra of ions such as Tl^+ , Pb^{2+} , and Bi^{3+} to probe the availability of electrons in the

¹ Interestingly enough, NaOH solutions of the same acid (H_2O) to (Na_2O) ratio as the most-studied Na_2O – SiO_2 solution, also have glass-forming ability and have been much used in low-temperature radiation chemistry studies.

oxides that provide the average environment of these probes to be donated to the probe ion orbitals. As with other indicators, each probe species is most useful for a certain range of basicity conditions. Duffy and Ingram used these spectra to establish a table of “optical basicities,” which have been used very effectively in assessing the relative basicities of a wide range of oxide melts (though precautions are needed when coordination changes occur, e.g., in peraluminous melts). The same probe ions have been used with comparable success to study the activity of chloride ions in molten chlorides [30, 31]. In this case, detailed electrochemical measurements of alkali chloride activities were available for comparison. Indeed, a semi-quantitative relationship between the free energy change across a given composition range from electrochemical measurements and that obtained from the change in orbital energies across the same composition range could be demonstrated [31].

Relationships similar to the above for silicate melts can similarly be drawn for the oxidic acid–base systems $\text{Na}_2\text{O} + \text{CO}_2$ (which give us the molten carbonate electrolytes of hydrocarbon-burning fuel cells) and for the other common glass-forming oxide systems $\text{Na}_2\text{O} + \text{B}_2\text{O}_3$ or P_2O_5 . A new system, currently under exploration in our research laboratory as a fuel cell electrolyte (Sun and Angell, to be published), bridges the gap between the borate and aqueous systems by employing an electrolyte containing the $\text{B}(\text{OH})_4^-$ anion, charge-compensated by tetraalkylammonium cations pendant to a polymer backbone.

Physically, distinctions between the siliceous and aqueous systems arise in different ways. The most important difference results from differences in coordinating abilities of the positively charged components Si^{4+} and H^+ of the respective Lewis acids. In the case of SiO_2 , both covalent and ionic bonding contributions require $\text{Si}(\text{IV})$ to be central to, and equally coordinated by, four oxygens. This results in a network of oxide-linked Si centers. In the case of H_2O , on the other hand, it is the oxygen that is coordinated by the positively charged species, and each oxygen is largely satisfied by the two covalently bonded protons of the isolated molecule. The “network” formed by the relatively weak coordination (through hydrogen bonds) of H^+ species on neighboring molecules is highly disrupted at ambient temperatures with the result that these acid–base systems are liquid at normal temperatures. The strong network of SiO_2 , by contrast, is only degraded above 1,200 °C, and its fragments carry ionic charges so that siliceous systems only exhibit fluid behavior at very high temperatures. While this circumstance leads to gross physical differences between the two systems, the chemical similarity remains.

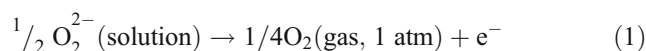
The different coordinating characteristics of H^+ and Si^{4+} may, however, be used to generate an essentially chemical difference between the two systems. The maximum coordination of oxygen by silicon is 2, and this is true also

for all the other common inorganic Lewis acid cations (B^{3+} , etc.) except H^+ . The oxygen of the OH_2 molecule can accept a third H^+ . The addition of the third proton causes a further polarization of the oxygen and thus produces a further large drop in the thermodynamic activity of the oxide ion [in the vicinity of the (neutral) H_2O stoichiometry] for which no parallel exists in the siliceous systems.² It is, of course, in the vicinity of this stoichiometry that most aqueous chemistry is actually performed.

With this outline of the chemical relationship between aqueous and other oxidic systems, let us point out similarities in the sort of solution chemistry problems, which are faced by those interested in such solutions, and then outline a scheme within which problems involving changes of oxidation state can be treated equivalently for all systems.

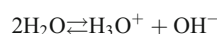
Two important classes of problems that are given attention by both aqueous and glass chemists are (1) the assessment of structural arrangements of solvent species around solute species [e.g., how many OH_2 , OH^- , or $^- \text{O}-\text{Si}-$ species are there in the first coordination shell of $\text{V}(\text{III})$, $\text{Nd}(\text{III})$, etc.?] and (2) the energetics of electron transfers between solute and solvent species [e.g., will $\text{V}(\text{II})$ be stable in a given oxide medium? Will Fe occur as $\text{Fe}(\text{II})$ or $\text{Fe}(\text{III})$ in a given laser glass?]. The answers to particular cases of each class prove to be rather sensitive to the value of a_{oxide} in all of the oxidic media. Similarities between redox processes in aqueous and molten oxide systems and between cation coordination schemes have often been noted, but quantitative relationships are rarely established.

An essential aspect of this paper is to re-emphasize the point that was central to the development in [7], viz., that redox problems in all these oxidic media can be reduced to a common basis by organizing our thinking (and our experimental data from spectroscopy, from chemical analysis, and from electrochemistry) around the reference electron transfer process

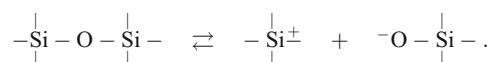


which is common to all systems.

² In the SiO_2 system, the nearest parallel of the autoionization of H_2O



is the bond cleavage



The equilibrium constant is of the order $e^{-(105 \text{ kcal})/RT} = 2 \times 10^{-22}$ at 1,000 K; $K_w \approx 10^{-14}$ at 298 K. In contrast to water, where HCl , etc. can be added to form H_3O^+ ($+\text{Cl}^-$, etc.), there is no external source of $-\text{Si}^{\pm}$ by means of which this equilibrium can be displaced to reduce $[\text{O}-\text{Si}-]$.

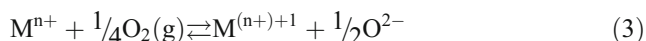
A secondary point is to demonstrate that the composition dependences of redox processes in oxidic media share a common feature. They are all, at first sight, anomalous and can only be understood if it is assumed that electron transfers away from solute species do not occur as independent processes but rather occur in concert with transfer of oxide species (or at least oxide electron density) to the new higher oxidation number species. Physically, this is to be recognized as an increased polarization of the solvent medium by the higher oxidation number cation. Most of the ideas presented in this paper were developed long ago in more detail in a discussion of the visible spectra of vitreous solids in [7].

The oxide–oxygen reference, electron transfers, and EFEL diagrams for individual solvents

In an oxidic solution in equilibrium with one atmosphere of oxygen, the distribution of a metallic element M between different valence states M^{n+} and $M^{(n+)+1}$ is determined by the reversible work expended to promote the transfer of a single electron from the reduced state to the gaseous oxygen species, according to

$$K_{\text{EQ}} = e^{-\varepsilon/kT} \quad (\text{cf. } N\varepsilon = \Delta G = -RT \ln K_{\text{EQ}}) \quad (2)$$

where K_{EQ} is the equilibrium constant for the exchange process



Normally, the oxide ion will not be stable as such but will react either with a solvent species such as $-\text{Si}-\text{O}-\text{Si}-$, H_2O , etc. to give $-\text{Si}-\text{O}^-$, OH^- , etc. species or with the oxidized species itself, but these are matters to be discussed later. Considering a solvent chosen to have unit activity of oxide and considering dilute solution standard states for the redox species such that activities can be replaced by mole fractions, K_{EQ} in Eq. 2 reduces to the concentration ratio of the two species. In such a solution, the free energy of electron transfer can be simply determined from a chemical or spectroscopic analysis of the redox ratio. As Gurney [8] has emphasized, it is the quantity ε that is characteristic of the process; the equilibrium constant that we observe is only a quantity, which, when taken as a logarithm and multiplied by $-kT$, provides a probabilistic (TdS) free energy change equal and opposite to ε , thus permitting dG to be zero for small transfers. This, of course, is the condition that defines an equilibrium state (hence Eq. 2). The quantity ε can be represented schematically by an analog of Gurney's diagram for proton transfer processes in aqueous solutions [8]. Figure 1 depicts ε as the interval between two levels in a diagram in which the oxidized and reduced states of the species are designated as "vacant" and "occupied" electron levels,

respectively. Thus we have, for the ferrous–ferric equilibrium, Fig. 1, see below.

From Fig. 1, we can see that electrons from an excess of Fe^{2+} species will "fall out" into the lower lying vacant levels on the O_2 species, thereby forming O^{2-} (or oxygen in the -2 oxidation state) and leaving behind Fe^{3+} . The electron dumping will proceed until $RT \ln K = -\varepsilon$, i.e., until the excess has been eliminated and equilibrium achieved.

If we were to choose the $\text{O}^{2-}(\text{soln})/\text{O}_2(\text{gas}, 1 \text{ atm})$ as a reference level, then the quantities ε for various electron transfer processes from reduced species to O_2 (or from O^{2-} to oxidized species) can be compared (1) with each other in the same solvent and (2) with themselves in other solvents to determine and interpret the influence of the medium on the electron transfer energy. Note that if the oxidic medium chosen were an $\text{Na}_2\text{O}+\text{H}_2\text{O}$ solution of Na_2O content equivalent to ~ 1 mol NaOH/kg , the quantity ε (eV) of Fig. 1 would be numerically equal to the aqueous solution standard oxidation potential for oxygen evolution less the standard oxidation potential for the $\text{Fe}(\text{II})/\text{Fe}(\text{III})$ electrode, i.e.

$$\varepsilon = -[E_{\text{B}}^{\text{O}}(\text{oxygen evolution}) - E_{\text{B}}^{\text{O}}(\text{Fe}(\text{II})/\text{Fe}(\text{III}))] \quad (4)$$

This relationship is depicted in Fig. 2, which we refer to as an electron free energy level (EFEL) diagram.

In practice, $\text{Fe}(\text{II})$ and $\text{Fe}(\text{III})$ are both precipitated from 1 M NaOH solution as solid hydroxides. In the equivalent $\text{Na}_2\text{O}+\text{SiO}_2$ solution, they remain in solution and can be also retained in the dissolved state in the glassy solid formed by cooling the melt to room temperature.

There are data of reasonable quality available for the concentration ratios K of a number of redox couples in the $\text{Na}_2\text{O}+\text{SiO}_2$ solvent of stoichiometry $\text{Na}_2\text{O}\cdot 2\text{SiO}_2$. These have been analyzed in some detail in [7], where an extensive comparison of the quantities ε derived using Eq. 1 was made with their aqueous solution equivalents obtained from Eq. 3 (except that the data for the aqueous media were for one molar acid solutions in which case there is no insolubility problem). To a lesser extent, redox ratios were investigated in sodium borate solutions [9, 32, 33]. In

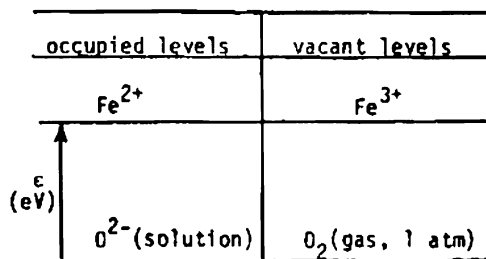


Fig. 1 Gurney representation of the energetics of transfer of an electron between the reduced Fe^{2+} state (ferric ion with an electron occupying its empty orbital) and gaseous oxygen to yield one half of an oxide ion and the oxidized Fe^{3+} state

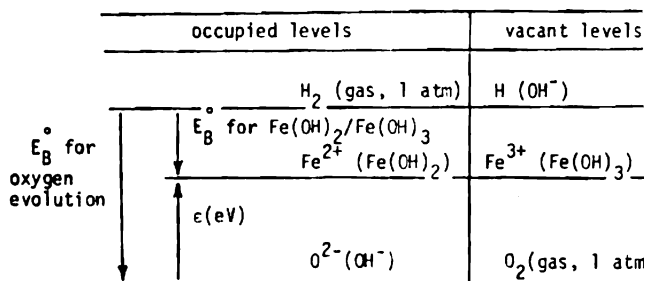


Fig. 2 Gurney diagram showing the relation of the energy ϵ of Fig. 1 to the standard oxidation potentials of aqueous solution chemistry

Fig. 3 (in separate columns), we show ϵ values for redox couples in the solutions $\text{Na}_2\text{O}\cdot 112\text{H}_2\text{O}$ (1 M NaOH) [34], $\text{Na}_2\text{O}\cdot 2\text{SiO}_2$ [8], and $\text{Na}_2\text{O}\cdot 2\text{B}_2\text{O}_3$ [8, 32, 33]. For comparison, the ϵ values for standard (~1 M) acid solutions, in which the oxide activity is 14 orders of magnitude lower than in the first of the above cases, are shown in the right hand diagram in Fig. 3. The energy level

sequences are generally rather similar in the different solvents, particularly in the siliceous and boraceous cases. In general, higher oxidation states appear to be more stable in the $\text{Na}_2\text{O}+\text{H}_2\text{O}$ solutions than in the others, which, as shown below, implies that H_2O is the weakest of the three Lewis acids considered in this study. The differences would be even more marked if the aqueous solutions were as rich in Na_2O as the siliceous and boraceous solutions.

In seeking to understand these differences, it should be remembered that (1) all that distinguishes the potential of a given ionic species in one solvent from that in another is the solvation free energy. From this, it follows that (2) the ϵ value of any redox couple relative to that for the same electron transfer process occurring in vacuum is determined by the difference in solvation free energies for the two states. Therefore, (3) differences between ϵ values for a given redox couple in different solvents reflect differences in the relative solvation free energies for the two members of the couple. Most generally, these differences seem to be

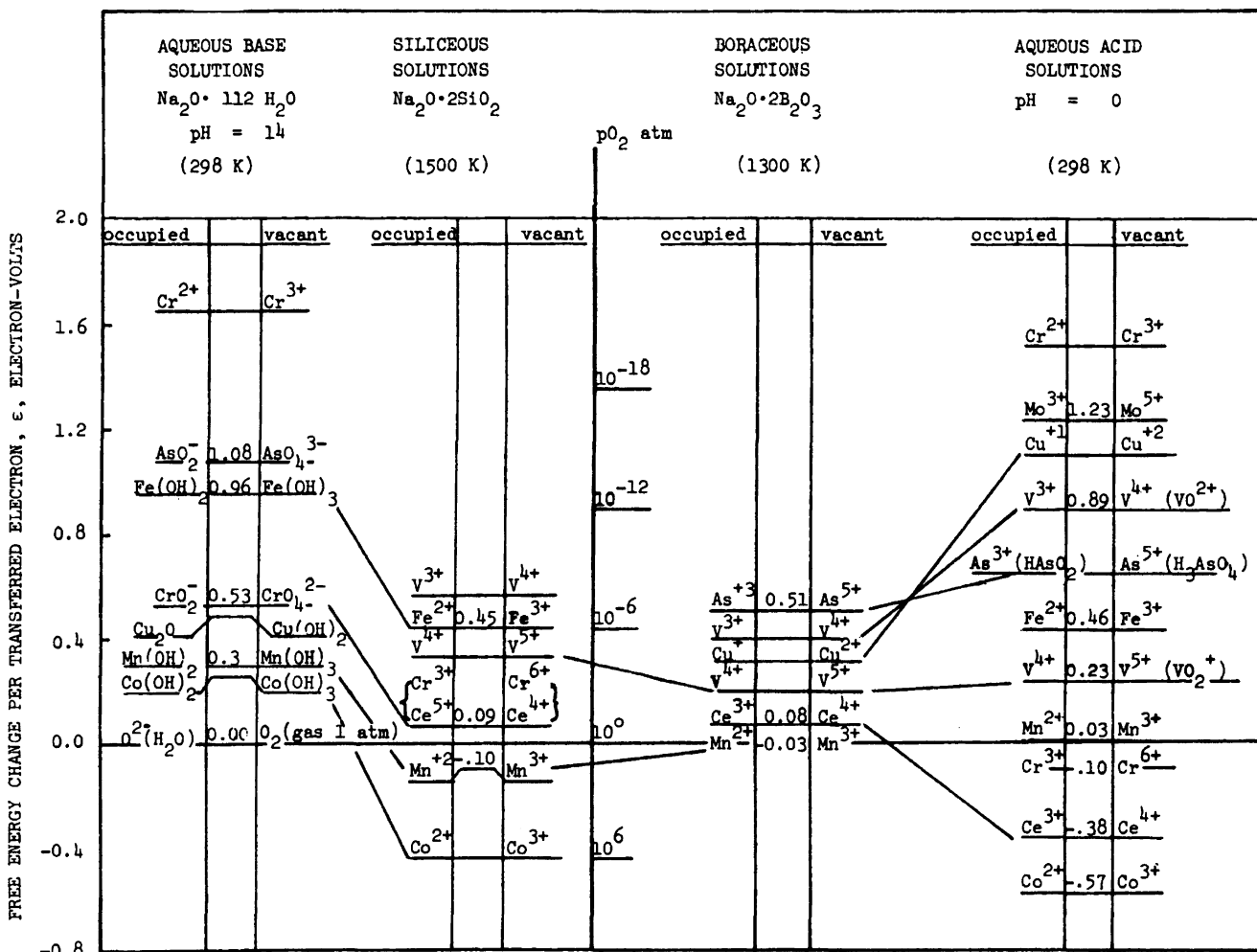


Fig. 3 Electron free energy level (EFEL) diagrams for redox couples in basic (LHS) and acid (RHS) aqueous solutions compared with levels for the same couples in siliceous ($\text{Na}_2\text{O}\cdot 2\text{SiO}_2$) and boraceous

($\text{Na}_2\text{O}\cdot 2\text{B}_2\text{O}_3$) solutions at the respective temperatures of equilibration. Reference level for all cases is the oxide/oxygen level at the same temperature

dependent on how effectively the higher oxidation state member of the couple competes with the solvent Lewis acid cation (H^+ , B^{3+} , Si^{4+} , P^{5+} , etc.) for the solvent oxygens. The more effective the competition, the greater the relative stabilization of the higher oxidation state in the solvent and the higher the ε value for the couple. Thus, high oxidation states are evidently best sought in aqueous systems (e.g., molten hydroxides), while low oxidation states will occur most generally in high P_2O_5 content solutions or their equivalent. The possibility, in the case of H_2O -containing solutions, of reducing the oxide ion activity seven orders of magnitude below that in the pure Lewis acid by the device of adding ~ 1 mol/l of H^+ ions (and thereby making a weak Lewis acid system appear relatively strong) clearly makes the aqueous medium a very versatile one for redox studies.

From the EFEL diagram, Fig. 3, the proportion of element M in the oxidized and reduced states in a given solution in equilibrium with 1 atm. of oxygen can be predicted using the relation

$$[OX]/[RED] = \exp(\varepsilon/kT) \quad (5)$$

where k has the value 8.62×10^{-5} eV K^{-1} if ε is in electron volt. Likewise, in a system in which exchange of electrons with O_2 gas is excluded, the distribution of redox species between two couples, e.g., Mn(II)/(III) and Fe(II)/(III), present in the same solution can be determined by Eq. 4 using, in place of ε , the difference in ε values between the individual couples.

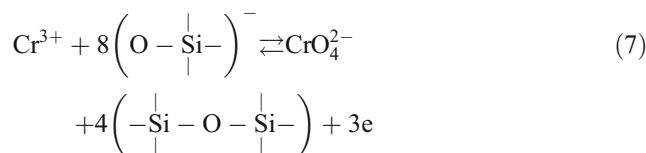
In most cases, a redox couple in solution will not be in equilibrium with oxygen at 1 atm. pressure. If $pO_2 = 0.21$ atm, as is often the case, the reference level is effectively shifted by $1/4kT$ in pO_2 ($=0.05$ eV), and 0.05 must be subtracted from ε in Eq. 5 before the redox ratio can be calculated [7]. If the oxygen pressure is deliberately lowered below 1 atm, e.g., by bubbling a 1:1 CO/CO_2 mixture ($pO_2 = 10^{-11}$ atm at 1,500 K) through the solution, then drastic changes in equilibrium distributions of oxidized and reduced species will occur. A pO_2 scale has been included in Fig. 3 to show the correction that must be made to the 1 atm O_2 electron transfer energy for solutions in equilibrium with atmospheres of lower and higher oxygen pressures (about 0.8 eV for CO/CO_2 equilibration). Such manipulations of the redox ratios are not often considered in aqueous solution chemistry (since gas-solution equilibria are usually only established very slowly) but could be of great importance in high temperature oxide solution chemistry. In practice, the oxygen pressure is often only crudely controlled, e.g., by adding carbonaceous material to the solution, with the result that predictions of final redox ratios are not easily made. Careful, controlled atmosphere, experimentation in this area of glass science has frequently been lacking.

Solvent composition effects, oxide transfers, and thermodynamic species

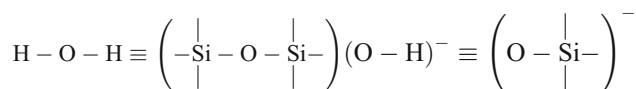
So far, we have considered only a single solvent composition in each of our three acid-base systems, Na_2O+H_2O , Na_2O+SiO_2 , and $Na_2O+B_2O_3$, (the aqueous acid case being distinct). Furthermore, we have, for convenience, assumed the activity of the oxide ion in Eq. 3 to be unity in each case (which can always be done by appropriate choice of standard state for the basic oxide). If we now attempt to predict from Eq. 3 the effect of changing solvent on the position of the redox equilibrium, we obtain contradictory results. For instance, increase of $[O^{2-}]$ by increase of Na_2O content should, in simple equilibrium thermodynamics, shift the equilibrium expressed by Eq. 3 to the left. In practice, such a solvent composition change generally leads to an increase in the proportion of the *higher* oxidation state. Similar observations in aqueous solutions were long ago rationalized by writing such electron transfer equilibria as



i.e., by incorporating the transfer of an oxide ion from a solvent species to the oxidized cation as an integral part of the electron transfer process. The strict equivalent of Eq. 6 in a silicate solvent would be

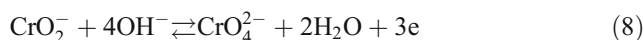


where the parallels



have been drawn (H^+ and Si^{4+} are the respective Lewis acid cations).

In aqueous solutions, the appropriate number of oxide transfers per electron transfer, n , is usually found to be about unity. Equation 7 implies the number $n = 1.33$, while the equilibrium in which the chromite ion CrO_2^- is recognized as the Cr^{+3} carrying species in basic solution, viz.,



implies the small number $n = 0.67$. In principle, the appropriate number can be obtained experimentally from the slope of the plot of ε vs $\log a_{OH^-}$ ($\log a_{OH^-} = pH - 14$), which is shown in Fig. 4a.

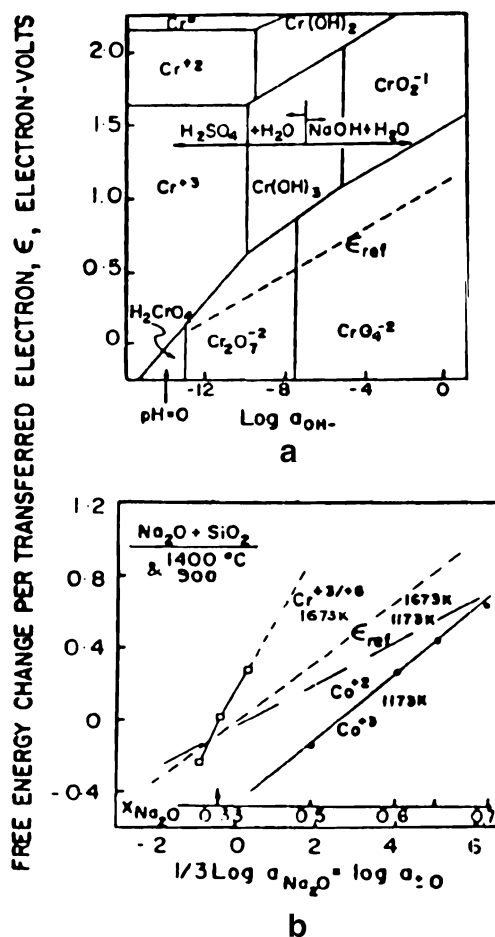
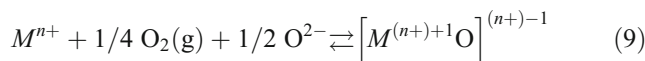


Fig. 4 **a** Free energy levels for stable chromium redox couples (referred to oxide/oxygen reference) as a function of hydroxide activity (log scale) in aqueous solutions at 298 K. **b** Free energy levels for $\text{Cr}^{3+}/\text{Cr}^{6+}$ and $\text{Co}^{2+}/\text{Co}^{3+}$ couples at 1,673 and 1,173 K, respectively, as a function of alkali oxide activity (log scale) in siliceous solutions

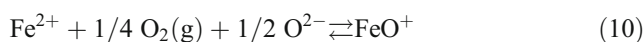
The argument is given in [7] and involves the assumption that correctly chosen species mix ideally so that an equilibrium constant, which is actually constant (and which therefore yields ε through Eq. 2), is obtained when K_{EQ} is written in terms of mole fractions. Figure 4a is in fact just the so-called Pourbaix diagram [35] for chromium in aqueous solutions transposed to show (1) oxidation potentials referred to the oxide/oxygen reference instead of reduction potentials referred to the H_2/H^+ reference on the vertical axis and (2) $\log a_{\text{OH}^-}$ instead of pH on the horizontal axis. Extraction of n from Fig. 4a requires knowledge of the variation of the reference level, ε for Eq. 2, with $\log a_{\text{OH}^-}$, which involves determination of the composition dependence of the OH^- activity. This is hardly a problem with aqueous solutions, and the reference slope is shown as a dashed line in Fig. 4a. On the other hand, determination of the dependence of basic oxide activity on composition is a major problem for molten oxides where experimentation is very difficult and where, in

consequence, results from different laboratories are often in disagreement.

In our original work [7], the data of Pearce [36, 37] for CO_2 solubility in $\text{Na}_2\text{O}+\text{SiO}_2$ melts were used, together with a standard state for the oxide solution defined by $\gamma_{\text{Na}_2\text{O}}=1.0$ at the composition $\text{Na}_2\text{O}\cdot 2\text{SiO}_2$ to construct a Pourbaix type diagram for the few redox couples, which have been studied quantitatively in molten oxides. A portion displaying the data for the $\text{Cr}^{3+}/\text{Cr}^{6+}$ equilibrium at 1,673 K (obtained by Nath and Douglas by chemical analysis of the quenched Cr-doped $\text{Na}_2\text{O}+\text{SiO}_2$ glasses) [10] is reproduced in Fig. 4b. The slope is greater than that shown for the $\text{CrO}_2^-/\text{CrO}_4^{2-}$ equilibrium in Fig. 4a and corresponds to 1.06 oxides transferred per electron transfer, i.e., $n=1.06$. Data plots for the $\text{Fe}^{2+}/\text{Fe}^{3+}$ and the $\text{Co}^{2+}/\text{Co}^{3+}$ equilibria in the same solvent system show somewhat smaller slopes [7] relative to ε (ref.) at the same temperature, yielding $n=0.8$. The general findings are thus approximately consistent with the thermodynamic equilibrium



a specific example of which would be



We will return to this conclusion with an interpretation of its physical significance after giving some consideration of the results of direct electrochemical studies on the redox equilibria quantified in Fig. 3.

Comparison with direct electrochemical measurements

Since the energy level diagrams of Fig. 3 were constructed in 1976, there have been few studies with which quantitative comparisons of the energy levels deduced in Fig. 3 can be made. Relative values are broadly consistent with those reported by Duffy and Ingram [28] using the most appropriate probe species [28, 29], but quantitative comparisons require electrochemical data on one or the other of the solvent systems in which the spectroscopic measurements have been made. This limits comparisons to a few of the data reported by von der Gönna and Rüssel [24], who reported square wave voltammetry studies on a variety of dilute redox couples dissolved in the liquid $\text{Na}_2\text{O}\cdot 2\text{SiO}_2$, over a range of temperatures common to those of the spectroscopic studies. We reproduce the summarizing figure from their work as Fig. 5 below.

In the study of von der Gönna and Rüssel, the current was measured as a function of increasing voltage with respect to a reference electrode reversible to oxygen gas at the dilution of ordinary air (ZrO_2/air electrode), which

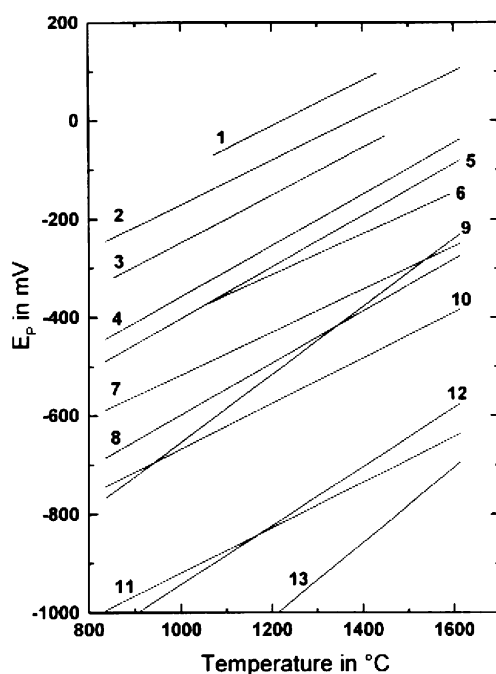


Fig. 5 Peak potentials from the square wave voltammetry study of Rüssel and von der Gönna [15] vs temperature (best fit line) for various multivalent redox pairs identified by numbers as follows: 1 $\text{Sb}^{5+}/\text{Sb}^{3+}$, 2 $\text{Cr}^{6+}/\text{Cr}^{3+}$, 3 $\text{Sn}^{4+}/\text{Sn}^{2+}$, 4 $\text{As}^{5+}/\text{As}^{3+}$, 6 $\text{Sb}^{3+}/\text{Sb}^0$, 7 $\text{As}^{3+}/\text{As}^0$, 8 $\text{V}^{5+}/\text{V}^{4+}$, 9 Cu^+/ Cu^0 , 10 $\text{Fe}^{3+}/\text{Fe}^{2+}$, 11 $\text{V}^{4+}/\text{V}^{3+}$, 12 $\text{Cr}^{3+}/\text{Cr}^{2+}$, 13 $\text{Ti}^{4+}/\text{Ti}^{3+}$. Note that the voltages are inverse to those of Fig. 3 due to the standard convention used in the plotting (such that least electronegative levels occur highest on the diagram)

establishes a potential slightly (0.05 eV) positive with respect to the pure oxygen reference level of the present work, as noted earlier. They report the peak voltage that corresponds to the voltage at midpoint of the total process in which an initially oxidized species is driven to the completely reduced state. At this midpoint, the redox ratio (equilibrium constant for the one electron transfer) is unity so the voltage corresponds to the value ε of Figs 2 and 3, except for the 0.05 eV correction due to the use of air rather than pure oxygen in the reference electrode. The sign of the voltage is reversed because we have chosen, following Gurney [8], to represent the electron transfer process as a physically appealing “falling” of electrons from high occupied energy levels down to the lower vacant levels on the reference species O_2 (gas), i.e., an oxidation, whereas Fig. 5 is constructed to accord with the conventional reduction potentials.

The results reported in Fig. 5 for the temperature 1,227°C are to be compared with those of Fig. 3, middle column, where they are seen to be generally in reasonable accord. For instance, the value for the couple $\text{Cr}^{3+}/\text{Cr}^{6+}$ of Fig. 3 corresponds to the value of curve 1 at 1,227°C, which is very close to zero: In Fig. 3, it is reported to be 0.09 eV with respect to pure oxygen. For $\text{Fe}^{2+}/\text{Fe}^{3+}$, our figure gives

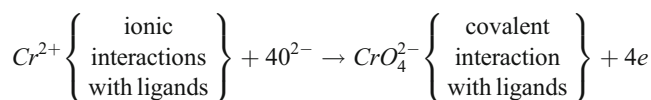
0.50 eV, whereas [15] reports 0.54 V. Considering the 40-year time difference between the studies, the agreement is quite pleasing.

The power of the direct electrochemical method to acquire data of good quality in short time is a clear advantage. The acquisition of data on the mean alkali oxide activity in alkali silicate melts, needed to confirm the interpretation of the oxide transfer process that accompanies the electron transfer (as described in the previous section), is eagerly awaited. We now review the physics of this process, as given in [7] and [23].

Interpretation of observed “oxide transfer” equilibria

Were Eq. 9 to be taken literally, one would expect to find Fe^{3+} in an oxide glass preferentially associated with one of its near-neighbor oxide ligands. While it is difficult to assess the exact coordination state of Fe^{3+} in oxide glasses because of a tendency to pass into fourfold coordination in basic solutions, the parallel case of Cr^{3+} is fairly unambiguous. Cr^{3+} can be viewed as arising through (1) an outward transfer to an electron from Cr^{2+} (which is known to exist in oxide solutions, was characterized spectroscopically by Paul [38]) plus (2) an inward transfer of an oxide ligand. It is found, by visible and electron paramagnetic resonance spectroscopic studies [7], to be coordinated symmetrically, Cr^{3+} lying at the center of an octahedron of oxide near neighbors. There is, in other words, no preferential attachment to one oxygen. It is strongly implied that the thermodynamic species M(III)O^+ suggested by the redox studies are not actual species and that Eqs. 8 and 9 require some other interpretation presumably involving electron density donation, as qualitatively argued by Duffy and Ingram [29].

We should first note that if three further electrons are transferred out from Cr^{3+} and three further “thermodynamic oxides” transferred in, the situation becomes better resolved, and the molecular ionic species CrO_4^{2-} can be identified spectroscopically. The spectrum of this species in the glass is, in fact, very similar to that of its well-known aqueous solution and inorganic salt counterpart. In such a case, we can write with some confidence



in which the thermodynamic and molecular models are consistent.

It is in the intermediate situation where electron transfer has occurred but no strong covalent bonds have been generated that the problem arises. The resolution lies in the

realization that wholesale transfer or electron density from molecular orbitals describing a single Si–O (or B–O, H–O) covalent bond into molecular orbitals of a metal-oxide covalent bond is unlikely for a +1 change in oxidation number unless there is some very specific molecular orbital structure favoring it (as in VO^{2+} cation formulation). What is more probable is simply that the cation in its higher oxidation state finds its electrostatic competitive status, vis-à-vis the solvent Lewis acid cation, incrementally improved and will proportionately counter-polarize the electron clouds of *all* its near neighbor anions. The net effect will be an adjustment in electron density around the oxidized species at the expense of that around several adjacent Lewis acid cations. The ion, in short, not only senses its electronic environment (optical basicity [28, 29]) but also alters it as it changes oxidation number. This incremental restoration of electron density to the oxidized species compensates for the stepwise loss of electron density, which occurs on increase of oxidation number, thus reducing the work of transfer of the electron away from the reduced species and, accordingly, raising the EFE level relative to the $\text{O}^{2-}/\text{O}_2(\text{gas})$ reference level.

The less available the ligand electrons are (i.e., the stronger the ligand binding by the Lewis acid cation), the lower the ϵ value for a couple and, accordingly, the greater the preponderance of low oxidation states for a given oxygen pressure. These conditions are those characteristic of strongly acid media. The limit is reached when there is no ligand electron density available at all, i.e., when the electron transfer is considered to occur in a vacuum.³ Conversely, the more polarizable the ligand, the greater the likelihood of observing higher oxidation states. Thus, the solutions in Fig. 3, in which water was the Lewis acid and H^+ the competing cation, were found to be those in which the ϵ levels were highest, hence those most predisposed to dump electrons from occupied levels (reduced species) into $\text{O}_2(\text{gas})$ vacant levels thereby creating higher-valent oxidized species at a given oxygen pressure. In short, aqueous NaOH solutions are the most favorable oxidation media of Fig. 3 (a–c) (at $p\text{O}_2=1$ atm) because H^+ is weak in the Lewis sense compared to B^{3+} and Si^{4+} . The conditions most favorable of all for the generation of high oxidation numbers in oxidic systems are, unfortunately, very corrosive and difficult to work with. Liquid hydroxides saturated with alkali oxides probably represent the most highly oxidizing oxidic solvent media conveniently available.

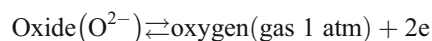
³ In practice such conditions are almost met in the so-called magic acid solutions in which the ligands are both intrinsically unpolarizable and also very strongly bound (as in SbF_6^-). We note that basic data exist from which this limiting, hence reference, EFEL diagram can be constructed.

The availability of oxide electron density to dissolved cations thus emerges as a primary solvent characteristic in redox chemistry. A related statement applies to the *coordination chemistry* of dissolved chemical species in a single and unchanging oxidation state (e.g., Co^{2+} , Ni^{2+}). It is shown in [7], for instance, that the same factors that promote high oxidation numbers in redox couples promote low coordination numbers for cations of variable coordination number.

The availability of ligand electrons can now be characterized conveniently and rather directly by optical methods following the work of Duffy and Ingram [29] and Reisfeld and Boehm [39], as briefly noted earlier. These workers showed that the energy of the $^1\text{S}_0 \rightarrow 3\text{P}_1$ transition of post-transition $d^{10}s^2$ metal ions, such as Tl^+ , Pb^{2+} , and Bi^{3+} , can be used as a sensitive probe of electron-donating properties of a solvent, i.e., of its basicity, and showed that the observed transition energies can be used to arrange solvent ligands into the same nephelauxitic series obtained originally from 3d ion spectral studies. In particular, Duffy and Ingram showed that these observations can be used to define an “optical basicity” scale in which a basicity value between 0 and 1 can be assigned to each solvent. The numbers obtained can be interpreted on the basis of theoretically derived microscopic basicities assigned to each ligand according to the species to which it is coordinated. The extent to which predictions of stable melt species and their spectroscopic properties can be made using these ideas remains to be fully documented, but clear parallels with thermodynamic findings were demonstrated in [29]. The optical approach has the advantage of specifying rather directly where the electrons should be and therefore what the spectroscopic consequences of changes in solvent system, or of changes in composition within a given solvent system, should be.

Summary

Similarities in the redox behavior of ions in oxide glasses (e.g., $\text{Na}_2\text{O}-\text{SiO}_2$, $\text{Na}_2\text{O}-\text{B}_2\text{O}_3$) and basic aqueous ($\text{Na}_2\text{O}-\text{H}_2\text{O}$) solutions quantitative basis by adoption of the



electron transfer process as a reference process of zero potential for all oxidic solutions. Data comparisons are made using EFEL diagrams. Differences in the free energy levels for redox couples dissolved in different types of oxidic solutions (aqueous, siliceous, etc.) obtained on this basis are related to the strength of the Lewis acid (H_2O , SiO_2 , and B_2O_3) of the solvent system. The composition dependence of the EFEL for a given couple in each solution

cannot be understood in terms of electron transfers alone. The thermodynamic data demand that “transfer in” of oxide ions from solvent to the oxidized species accompany the “transfer out” of the electron(s), approximately on a one-for-one basis. However, the “thermodynamic” species, such as CrO^+ , FeO^+ , etc. implied by such arguments, may not exist as such, since the same composition effect on the EFELs would follow from the “transfer in” of some oxide ligand electron densities from each of a number of ligands. The latter process is broadly consistent with the picture that was developed by Duffy and Ingram from optical basicity arguments.

Concluding remarks

While the developments reviewed above present a self-consistent basis for understanding the common features of redox chemistry in aqueous, hydroxidic, and liquid oxide solutions, much spectroscopic and thermodynamic investigation remains to be performed before the body of ideas and experimental observations contributing to the “oxidic solutions” subfield of solution chemistry can be properly consolidated. We note also that various aprotic molecular solvents like dimethyl sulfoxide coordinate redox species by oxygen ligands, and no attempt has been made in this study to incorporate them into the overall scheme. The rapidly growing field of ambient temperature ionic liquids (ILs) [40, 41] and in particular its protic IL (pIL) branch [42, 43] also awaits attention from redox chemists. More is likely to be heard of these systems in the immediate future.

Acknowledgment We are grateful for the support of the National Science Foundation under Grants from the NSF-DMR Solid State Chemistry branch.

References

- Bockris JO, Lowe DC (1954) *Proc R Soc Lond A Math Phys Sci* 226:423
- Bockris JO, McKenzie JD, Kitchener JA (1955) *Trans Faraday Soc* 51:1734–1748
- Bockris JO, Tomlinson JW, White JL (1956) *Trans Faraday Soc* 52:532–541
- Tomlinson JW, Heynes MSR, Bockris JO (1958) *Trans Faraday Soc* 54:1822–1833
- Bockris JO, Conway BE (1949) *Trans Faraday Soc* 45:989
- Salanne M, Simpson C, Turq P, Madden PA (2008) *J Phys Chem B* 112:1177–1183
- Wong J, Angell CA (1976) *Glass: structure by spectroscopy*, Chapter 6. Marcel Dekker, New York. <http://www.public.asu.edu/~caangell/>
- Gurney RW (1962) *Ionic processes in solution*. Dover Publications, New York
- Paul A, Douglas RW (1965) *Phys Chem Glasses* 6:207
- Nath P, Douglas RW (1965) *Phys Chem Glasses* 6:197
- Johnston WD (1964) *J Am Ceram Soc* 47:198
- Johnston WD, Chelko A (1966) *J Am Ceram Soc* 49:562
- Sasahari A, Yokokawa T (1985) *Electrochim Acta* 30:441
- Tilquin J, Duveiller P, Gilbert J, Claes P (1995) *J Non-Cryst Solids* 211:1997
- Rüssel C, von der Gönna G (1999) *J Non-Cryst Solids* 260:147–154
- de Strycker J, Gerlach S, von der Gönna G, Rüssel C (2000) *J Non-Cryst Solids* 272:131–138
- Benne D, Keding R, Rüssel C (2005) *J Non-Cryst Solids* 351:37–39
- van der Gönna G, Rüssel C (2001) *J Non-Cryst Solids* 288:175–183
- Paul A, Douglas RW (1967) *Phys Chem Glasses* 8:151
- Lin T-C, Angell CA (1984) *Commun Am Ceram Soc* 67:C33
- Couch TW, Smith GP (1970) *J Chem Phys* 53:1336
- Duffy JA, Ingram MD (2002) *Comptes Rendus Chimie* 5:797–804
- Angell CA (1977) In: Mamantov G (ed) *Spectroscopic and electrochemical characterization of solute species in non-aqueous solvents*. Plenum, New York, p 273
- von der Gönna G, Rüssel C (1999) *J Non-Cryst Solids* 260:147
- Duffy JA, Ingram MD (1971) *J Am Ceram Soc* 93:6448
- Duffy JA, Ingram MD (1971) *J Phys Chem* 54:443
- Duffy JA, Ingram MD (1974) *J Inorg Nucl Chem* 36:30
- Duffy JA, Ingram MD (1974) *J Inorg Nucl Chem* 36:42s
- Duffy JA, Ingram MD (1976) *J Non-Cryst Solids* 17:373
- Angell CA, Bennett PD (1982) *Inorg Chem* 104:3604
- Bennett PD, Angell CA (1985) *Inorg Chem* 24:3030
- Paul A, Douglas RW (1965) *Phys Chem Glasses* 6:212
- Bancroft W, Nugent RL (1929) *J Phys Chem* 33:481
- Latimer WM (1952) *The oxidation states of the elements and their potentials in aqueous solutions*, 2nd edn. Prentice Hall, New York
- Pourbaix, M (1966) *Atlas of electrochemical equilibria in Aqueous solutions*. Pergamon Press, Oxford
- Pearce ML (1964) *J Am Ceram Soc* 47:342
- Pierce ML (1965) *J Am Ceram Soc* 48:175
- Paul A (1974) *Phys Chem Glasses* 15:197
- Reisfeld R, Boehm L (1975) *J Non-Cryst Solids* 17:209
- Rogers RD, Seddon KR (2003) *Science* 302:792–793
- MacFarlane DR, Pringle JM, Johansson KM, Forsyth SA, Forsyth M (2006) *Chem Commun* 18:1905–1917
- Belieres J-P, Angell CA (2007) *J Phys Chem B* 111:4926–4937
- Greaves TL, Drummond CJ (2008) *Chem Rev* 108:206–237